



Wave energy hotspots - a numerical study of wave processes at Belharra, South West of France

Diego SLAMOVITZ¹, Matthias DELPEY², Denis MORICHON¹,
Stéphane ABADIE¹, Mario MORALES-HERNÁNDEZ³,
Peyo LIZARAZU, Volker ROEBER¹

1. Université de Pau et des Pays de l'Adour, E2S-UPPA, SIAME, 64600 Anglet, France.
dslamovitz@univ-pau.fr; denis.morichon@univ-pau.fr; stephane.abadie@univ-pau.fr;
volker.roeber@univ-pau.fr
2. SUEZ Eau France, Rivages Pro Tech, 64210 Bidart, France.
matthias.delpey@suez.com
3. University of Zaragoza, I3A, 50001 Zaragoza, Spain.
mmorales@unizar.es

Abstract:

Highly energetic swells occasionally produce unusually large surf at Belharra, a famous rock formation at the French Basque coast, near St. Jean de Luz. This work attempts to better understand the underlying processes that lead to extreme wave heights at this location. Here, we use a combination of a spectral wave model, SWAN, and a phase-resolving model, BOSZ, to study how variations in offshore swell conditions and tide levels affect the regional and local wave fields. We carry out a detailed wave-by-wave investigation of the local conditions for a wide range of plausible, highly energetic scenarios, and draw qualitative comparisons with data from the trajectory of a surfer riding a wave at Belharra. In general, regional and local patterns in the bathymetry seem to control the concentration of swell energy towards this spot. Large wave periods and swell directions around 300° - 310° generate the most energetic local conditions. Higher tide levels lead to overall taller waves, albeit with weaker breaking intensities.

Keywords:

Ocean waves modeling, Surf-zone processes, Breaking waves, Boussinesq-type model, Spectral model, Extreme waves.

1. Introduction

Belharra is a world-renowned big wave surfing spot situated 2.5 km off the Socoa cliff, at the French Basque coast. It lies above an underwater rock formation which is 15 m deep in its shallowest section. Thus, very energetic swells are required for waves to break here. This does not occur often, even if the region frequently encounters highly energetic swells, especially during winter time. Typical winter swells at this location exhibit significant wave heights (H_s) from 2 m to 5 m with peak periods (T_p) from 10 s to 15 s (ABADIE *et al.*, 2005; LASTIRI *et al.*, 2020). Situated in a meso-tidal area, the highest spring tide range reaches approximately 4 m (ABADIE *et al.*, 2006).

Peyo Lizarazu (depicted in Figure 1) - a local big wave surfer and Belharra pioneer - recently recorded his trajectory while surfing at this location during a big swell event. This study includes qualitative comparisons between numerical results and this field data. Furthermore, this work aims to deepen the understanding of the wave dynamics at this spot, including the factors contributing to their extreme heights and their effects on nearby processes. We examine the specific conditions that lead to the formation of extreme waves, employing numerical simulations to observe how the wave field responds to various combinations of swell conditions and tide levels. Utilizing a combination of a spectral model and a phase-resolving model for coastal and local conditions respectively, we investigate significant wave height, free surface elevation over time, and turbulent kinetic energy (TKE) for each scenario.



Figure 1. Peyo Lizarazu surfing Belharra, February 2011 (photo: Bonnarme).

Our focus is on large open ocean swells. As waves move from deep to shallow water, they undergo transformations due to interactions with the seafloor. Shoaling causes waves to slow down and shorten in length that consequently leads to an increase in height. Refraction further modifies their trajectory in shallower waters, aligning their crests more closely with the seabed contours. In the presence of heterogeneous bathymetries, refraction can generate convergence of the wave energy towards local shallows, amplifying wave heights and causing significant variations in breaker height along the coast. These processes, along with wave breaking, significantly affect coastal dynamics,

including long-shore currents, rip currents, and mixing (MUNK & TRAYLOR, 1947; CHOI *et al.*, 2015).

Key parameters for evaluating surf quality include wave height, breaker shape, and intensity. The breaker shape can be categorized based on the Iribarren number (ξ), with waves classified as spilling for $\xi < 0.4$, plunging for $0.4 < \xi < 2.0$, and surging/collapsing for $\xi > 2.0$ (GALVIN, 1968; MEAD & BLACK, 2001).

2. Methodology

2.1 Modeling setup

We run a large number of computations to analyze how offshore incident wave conditions and tide levels affect the wave field at Belharra. We use a spectral model, SWAN (BOOIJ *et al.*, 1999), and a phase-resolving model, BOSZ (ROEBER, 2010), for the computations in the coastal and local scales respectively. Considering we are interested in the most energetic range of conditions that occur in the region (the scenarios that are likely to produce big surf at Belharra), we compute cases combining the offshore swell parameters in the following ranges: H_s in [3 m, 8 m], T_p in [12 s, 20 s], D_p (peak direction) in [275°, 345°]. The still water level is set to 1 m above chart datum, except for the cases in which the effect of the tide is studied - for this, we consider water levels varying from 0 to 4 m.

2.1.1 SWAN setup

We use a 25 km by 20 km SWAN domain with a uniform grid of square cells, 100 m side length, and bathymetric data from SHOM. The offshore conditions are set along the north and west boundaries of the domain as Pierson-Moskowitz spectra. Each case is run until getting its stationary solution. These computations provide the frequency-direction wave energy spectra along the offshore boundary of the BOSZ domain, that is used as input for the BOSZ wave-maker.

2.1.2 BOSZ setup

In BOSZ, we use a 3.5 km by 4 km domain, with uniform square grid cells of 5 m. The domain is oriented so that the offshore boundary is approximately aligned with D_p . We use a Manning coefficient of $0.02 \text{ sm}^{-1/3}$ for the seabed, and a Courant number of 0.5. A uniform depth of 35 m for the first 500 m of the domain ensures validity of the wave-maker. Sponge layers on all boundaries absorb the outgoing wave energy.

Since BOSZ is a depth-integrated model, it cannot describe overturning of the free surface, thus wave breaking is always an approximation (ROEBER & CHEUNG, 2012). The criteria used here is based on the free surface Froude number (F_{rs}) - the ratio between particle speed at the free surface and wave celerity in shallow water. It considers that waves break when F_{rs} exceeds 0.9, which seeks to represent that the particle speed at their top is greater than the speed of the entire wave. Though this technically happens

Thème 1 – Hydrodynamique marine et côtière

when $Fr_s > 1$, it has been proven that when Fr_s reaches 0.85 the wave has passed the point of no return and will eventually break shortly after (VARING *et al.*, 2021). When the threshold is reached, TKE is produced. It is used for the computation of eddy viscosity in a diffusive term added to the momentum equations, mostly active along the wave breaking front, so the free surface cannot develop a sharp shock-front. This prevents the dispersion terms from pumping excessive amounts of energy into the wave face and causing a blow-up (ZELT, 1991; ZHANG *et al.*, 2014). A one-equation model is used to determine the spatial and temporal variations of TKE, considering its advection, destruction, production, and diffusion (NWOGU, 1996). Though TKE is produced locally where the breaking criteria is exceeded, it can remain in the system for some time and be transported. It can be seen as virtual whitewater, where the induced turbulence from breaking waves gradually diminishes (KALISCH *et al.*, 2023).

2.2 Qualitative comparison with geolocation data

SWAN and BOSZ have shown to provide accurate results in various scenarios (BOOIJ *et al.*, 1999; ROEBER & CHEUNG, 2012; PINAULT *et al.*, 2022). However, their capability to accurately reproduce reality at Belharra remains uncertain due to the complexity of the problem. Peyo Lizarazu provided records from his GPS-equipped watch of his latitude, longitude and altitude while surfing at this location. In the absence of any other field measurements in this site so far, this unusual data offers a qualitative tracking of a breaking wave front, which allows for comparisons with the numerical results. We do not intend to replicate the exact wave that the surfer rode, nor is this an attempt to validate the numerical models. However, comparing the results of the model with the surfer's track provides a preliminary insight into the realism of the simulated wave breaking locations.

3. Results

3.1 Influence of the offshore incident swell conditions and tide level

Results from the SWAN computations in the coastal domain show that waves off Belharra are taller than in their surroundings, to an extent of around 15 km, as shown in Figure 2 (left). Which reveals the presence of a wave energy focusing zone in this area. We notice changes in the direction of the swell when it travels through the coastal domain, strongly depending on the incident D_P and T_P , but independent of H_s . As shown in Figure 2 (right), swells from more western directions are refracted towards the south (positive shift), and swells from more northern directions are refracted towards the east (negative shift). In all cases, their direction becomes closer to around 320° . Although less important than the influence of the swell direction, that of the period is also considerable. The refraction and consequently the change of the peak direction tends to be stronger for larger periods.

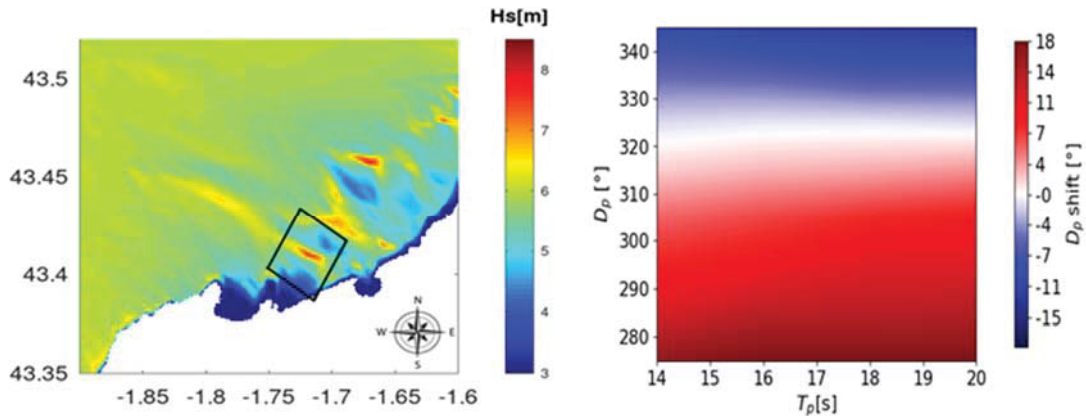


Figure 2. SWAN results. Left: coastal field of H_s [m], for offshore conditions $H_s=6m$, $T_P=16s$, $D_P=305^\circ$. The black rectangle illustrates the limits of the BOSZ domain for this case. Right: D_P shift [°] from the offshore boundary of the SWAN domain to the offshore boundary of the BOSZ domain, for offshore $H_s=6m$.

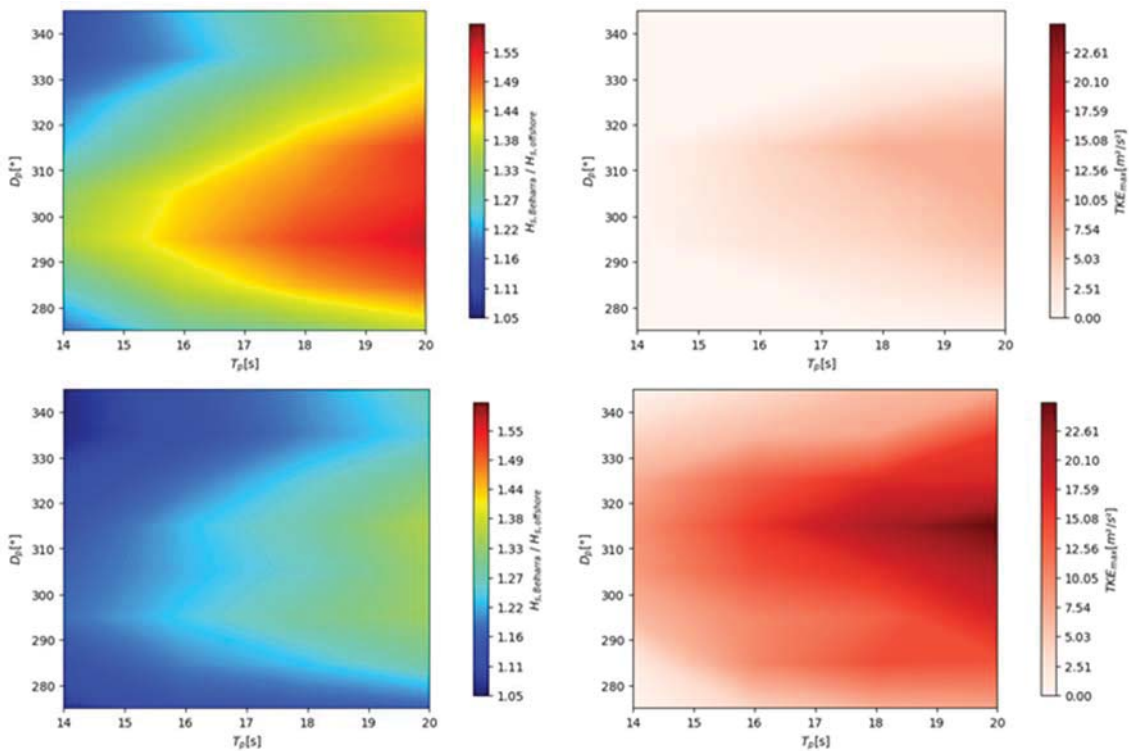


Figure 3. Left: wave amplifications at the site of interest. Right: maximum TKE values at the site of interest [m²/s²]. Top: offshore $H_s=5m$. Bottom: offshore $H_s=7m$.

For each case and for each time frame, we extract the maximum TKE value in the whole domain. Analyzing its evolution in time, we note repeated patterns of increases and subsequent decreases. These correspond to waves coming in groups - we confirm this by looking at the evolution in time of the free surface elevation computed with BOSZ. We generally identify sets of 1 to 3 waves, arriving every 200 s to 300 s. We use the maximum

Thème 1 – Hydrodynamique marine et côtière

TKE values in each simulation as indicators of the wave breaking intensity, to compare different cases.

As illustrated in Figure 3, the wave amplifications and TKE production increase with T_P . These two parameters are strongly correlated with T_P , with Pearson correlation coefficients of 0.98 and p-values around 0.00 in both cases. TKE is produced only for periods above 15 s. Also shown in Figure 3, swell directions closer to around 300° produce larger wave amplifications, and swell directions closer to around 315° produce higher TKE values. The results also reveal that taller waves produce more TKE, but are less amplified.

Though waves are classified as plunging for all cases, ξ values at Belharra increase with the period, and with more northern D_P values; and they decrease with H_s and the tide level.

As Figure 4 depicts, when the still water level increases, wave amplifications increase but TKE values decrease. Both of the order of 5% for every meter of tidal elevation, with respective Pearson correlation coefficients of 0.97 and 0.94, and p-values around 0.00 and 0.01.

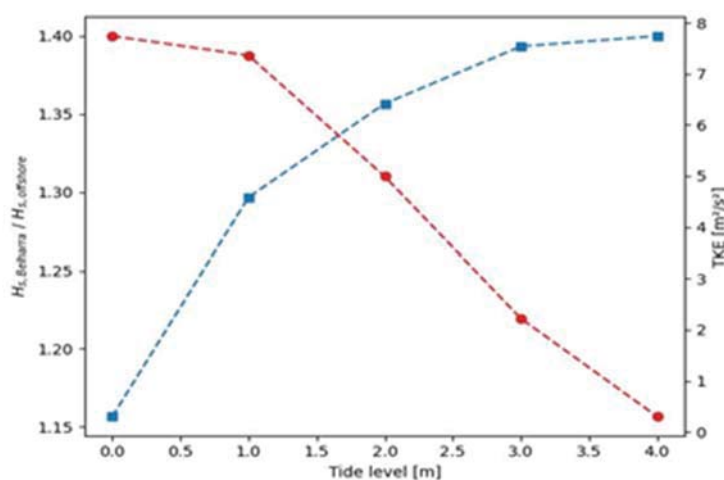


Figure 4. Wave amplifications (blue) and TKE values [m^2/s^2] (red) dependence on tide level [m]. For offshore $H_s = 6m$, $T_P = 16s$ and $D_P = 305^\circ$.

3.2 Qualitative comparison with geolocation data

Although we do not know the exact conditions when the geolocation data was recorded, we draw comparisons between the surfer's trajectory and waves from computed scenarios that are likely to produce big surf according to the previous analysis. We expect the surfer to be close to the breaking part of the wave, right ahead of the crest and the right end of the TKE trace (when riding a lefthander wave). For some computed waves, the agreement with the field data is remarkable. Figure 5 presents the recorded trajectory superimposed over the free surface elevation and TKE trace for one of these cases. The records coincide

with the expected position according to the simulation for 15-20 s. Then the surfer progressively moves ahead of the wave, around the time when the TKE production stops. If we consider that waves can be surfed when they break, i.e. when TKE is produced, this ride would be around 230 m long. The recorded variation in altitude is 11.8 m - it increases for the first 16 s and then decreases. As a comparison, the height of the computed wave depicted in Figure 5 is 13.3 m (obtained using a zero-crossing method). The average horizontal speed recorded by the surfer starts at 13.0 m/s, increases until 24.8 m/s, and finally slows down until 19.1 m/s. The average wave speed in the simulation is around 12.5 m/s.

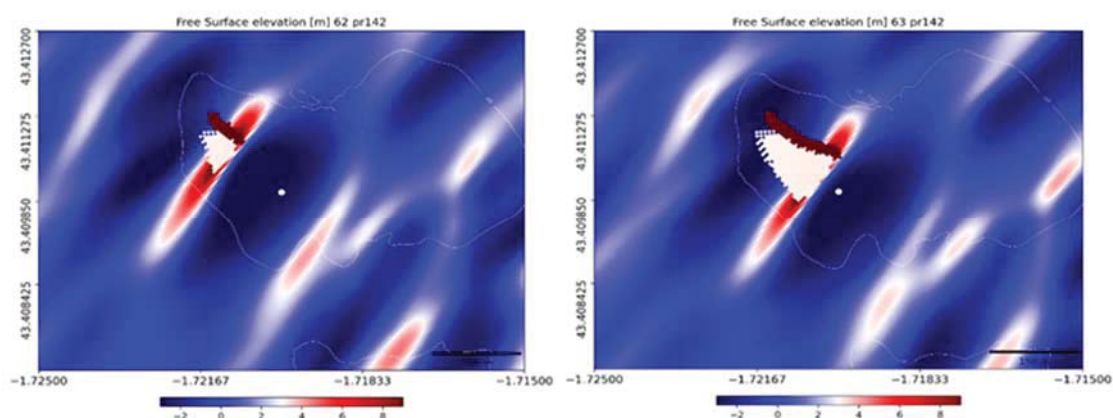


Figure 5. Dark red: evolution in time of the surfer's trajectory. Blue to red scale: free surface elevation. White trace: TKE non-null. For offshore $H_s = 6\text{m}$, $T_P = 16\text{s}$ and $D_P = 315^\circ$. Difference in time between right and left Figures: 5 s.

4. Discussion and conclusions

The mechanics of Belharra appear to be driven by the bathymetry, both on a regional and local scale. Regionally, we identified a ridge standing out of the nearshore area and pointing right towards Belharra, from around 300° . It is approximately 60 m deep initially, surrounded by depths of more than 90 m, and extends for roughly 20 km until reaching the seamount where waves finally break. This feature almost overlaps a region where H_s is significantly larger than in the surrounding area (shown in Figure 2). Its orientation is close to that at which the swell direction is refracted, and therefore favors energy concentration. This ridge seems to play a fundamental role in the refraction of swells and the concentration of the wave energy at Belharra. This shows that the processes leading to giant waves at this location begin far offshore, consistent with their effect being more significant for higher periods. Locally, a rock formation, considerably shallower than its surroundings, leads the waves to grow to huge heights and finally triggers their breaking with extreme intensity.

Swell directions around $300^\circ - 310^\circ$ favor the concentration of energy at Belharra the most. Within this directional window, the western end produces larger wave

Thème 1 – Hydrodynamique marine et côtière

amplifications, whereas the northern end produces more intense wave breaking. Wave amplifications and breaking intensities increase with the swell period. For taller waves, the breaking is more energetic but less sudden, and wave amplifications are weaker - since waves break earlier, they have less time to grow beforehand. Something similar happens when the tide decreases: there is more wave breaking and it occurs earlier, thus wave amplifications are weaker.

The Frs breaking criteria was developed for low Reynolds flows in pipes: very different conditions than those we are studying. Plus, we could have used a slightly different threshold, as explained in Section 2. Although this adds an error, as far as this study goes, we cannot discern its importance. In this regard, it could be useful to use other breaking criteria and compare the results.

The trajectory documented by Peyo Lizarazu appears qualitatively plausible. He gains speed and altitude before taking off, then accelerates and loses altitude while riding the wave, outpacing it, and slowing down afterwards. Quantitatively, the trajectory seems fast, even though we expect the speed to be high, considering the water depth. The shallow water approximation would be 12.1 m/s (for a depth of 15 m). The average wave speeds in the simulations seem more plausible. Still, the qualitative comparison with the numerical results shows that the location of the breaking in the computations seems realistic. For some cases, the surfer's position is remarkably similar to that expected from the computations. Added to all the realistic patterns found, this suggests that the numerical models, the parameterization and the whole methodology used, seem to be capable of fairly reproducing what happens at Belharra. This motivates further investigation to validate the methods through detailed quantitative comparisons with more observations, either in the field or from remote sensing. We are also keen to carry out similar studies for other spots, and draw comparisons between them.

Acknowledgments

This study was carried out in the framework of the E2S chair HPC-Waves and the Laboratoire Commun KOSTARISK. The authors acknowledge financial support from the I-SITE program Energy & Environment Solutions (E2S), the Communauté d'Agglomération Pays Basque (CAPB), and the Communauté Région Nouvelle Aquitaine (CRNA) for the E2S chair HPC-Waves. The project has received funding from the European Union's Horizon 2020 research and innovation programme under the Marie Skłodowska-Curie grant agreement No 945416.

5. References

ABADIE S., BUTEL W., DUPUIS H., BRIERE C. (2005). *Statistical parameters of waves on the south Aquitaine coast*. Comptes rendus geoscience, Vol. 337, No. 8, pp. 769–776. <https://doi.org/10.1016/j.crte.2005.03.012>

- ABADIE S., BUTEL R., MURIET S., MORICHON D., DUPUIS H. (2006). *Wave climate and longshore drift on the south Aquitaine coast*. Continental Shelf Research, Vol. 26, No. 16, pp. 1924–1939. <https://doi.org/10.1016/j.csr.2006.06.005>
- BOOIJ N., RIS R.C., HOLTHUIJSEN L.H. (1999). *A third-generation wave model for coastal regions: 1. Model description and validation*. Journal of geophysical research: Oceans, Vol. 104, No. C4, pp. 7649-7666. <https://doi.org/10.1029/98JC02622>
- CHOI J., KIRBY J. T., YOON S.B. (2015). *Boussinesq modeling of longshore currents in the Sandy Duck experiment under directional random wave conditions*. Coastal Engineering, Vol. 101, pp. 17-34. <https://doi.org/10.1016/j.coastaleng.2015.04.005>
- GALVIN C. (1968). *Breaker type classification on three laboratory beaches*. Journal of geophysical research, Vol. 73, No. 12, pp. 3651–3659. <https://doi.org/10.1029/JB073i012p03651>
- KALISCH H., LAGONA F., ROEBER V. (2023). *Sudden wave flooding on steep rock shores: a clear but hidden danger*. Natural Hazards, pp. 1-21. <https://doi.org/10.1007/s11069-023-06319-w>
- LASTIRI X., ABADIE S., MARON P., DELPEY M., LIRIA P., MADER J., ROEBER V. (2020). *Wave energy assessment in the south Aquitaine nearshore zone from a 44-year hindcast*. Journal of Marine Science and Engineering, Vol. 8, No. 3, 199. <https://doi.org/10.3390/jmse8030199>
- MEAD S., BLACK K. (2001). *Field studies leading to the bathymetric classification of world-class surfing breaks*. Journal of Coastal Research, pp. 5–20. <https://www.jstor.org/stable/25736201>
- MUNK W. H., TRAYLOR M. A. (1947). *Refraction of ocean waves: a process linking underwater topography to beach erosion*. The Journal of Geology, Vol. 55, No. 1, pp. 1–26. <https://doi.org/10.1086/625388>
- NWOGU O.G. (1996). *Numerical prediction of breaking waves and currents with a Boussinesq model*. Coastal Engineering, pp. 4807-4820. <https://doi.org/10.1061/9780784402429.374>
- PINAULT J., MORICHON D., DELPEY M., ROEBER V. (2022). *Field observations and numerical modeling of swash motions at an engineered embayed beach under moderate to energetic conditions*. Estuarine, Coastal and Shelf Science, Vol. 279, pp. 108143. <https://doi.org/10.1016/j.ecss.2022.108143>
- ROEBER V. (2010). *Boussinesq-type model for nearshore wave processes in fringing reef environment*. Doctoral thesis, University of Hawaii at Manoa.
- ROEBER V., CHEUNG K. (2012). *Boussinesq-type model for energetic breaking waves in fringing reef environments*. Coastal Engineering, Vol. 70, pp. 1–20. <https://doi.org/10.1016/j.coastaleng.2012.06.001>
- VARING A., FILIPOT J.-F., GRILLI S., DUARTE R., ROEBER V., YATES M. (2021). *A new definition of the kinematic breaking onset criterion validated with solitary and quasi-regular waves in shallow water*. Coastal Engineering, Vol. 164, pp. 103755. <https://doi.org/10.1016/j.coastaleng.2020.103755>

Thème 1 – Hydrodynamique marine et côtière

ZELT J. (1991). *The run-up of nonbreaking and breaking solitary waves*. Coastal Engineering, Vol. 15, No. 3, pp 205–246. [https://doi.org/10.1016/0378-3839\(91\)90003-Y](https://doi.org/10.1016/0378-3839(91)90003-Y)

ZHANG Y., KENNEDY A.B., DONAHUE A.S., WESTERINK J.J., PANDA N., DAWSON C. (2014). *Rotational surf zone modeling for $O(\mu^4)$ Boussinesq–Green–Naghdi systems*. Ocean Modelling, Vol. 79, pp. 43–53. <https://doi.org/10.1016/j.ocemod.2014.04.001>